

Interplay between Oxidation State and Coordination Geometry of Metal Ions in Azurin

Rogert Bauer,* Eva Danielsen, Lars Hemmingsen, Morten J. Bjerrum,[†]
Örjan Hansson,[‡] and Kulwant Singh[§]

Contribution from the Department of Mathematics and Physics, Royal Veterinary and Agricultural University, DK-1871 Frederiksberg C, Denmark

Received July 18, 1996[⊗]

Abstract: The small electron transporting copper protein, azurin, has been studied in order to investigate the interplay between the oxidation states of the metal and its coordination geometry. The results show that the metal coordination geometry for Ag(I) in Ag(I) substituted wild type azurin is only slightly different from the geometry for Cd(II) in cadmium substituted azurin both being similar to the geometry for copper in native azurin. Furthermore, the coordination geometry for Ag(I) in the Met121 to Leu substituted mutant of azurin is also similar to the geometry of copper in native azurin. In contrast, previously published results show that Cd(II) substituted Met121Leu-azurin exhibits two different coordination geometries for Cd(II), one again similar to the wild type geometry and another very flexible and distinctly different from wild type azurin. These results have been obtained by Perturbed Angular Correlation of γ -rays spectroscopy using the two radioactive isotopes $^{111}\text{Ag(I)}$ and $^{111\text{m}}\text{Cd(II)}$ as probes of a monovalent and a divalent ion, respectively. The technique also revealed that the metal-coordination geometry for Ag(I) in wild type azurin relaxes to the coordination geometry of Cd(II) on a time scale of 100 ns after the decay from $^{111}\text{Ag(I)}$ to $^{111}\text{Cd(II)}$. We suggest that the role of Met121 is to maintain the rigid tricoordinated metal coordination geometry independent of the oxidation state of the metal.

Introduction

Change of oxidation state of the copper ion is a key feature in electron-transporting copper proteins, and there is a strong interest in studying the interplay between protein and metal ion in both oxidation states. We publish here for the first time results using PAC (Perturbed Angular Correlation of γ -rays) spectroscopy with $^{111}\text{Ag(I)}$ incorporated in azurin. These results combined with previously published results from PAC spectroscopy with $^{111\text{m}}\text{Cd(II)}$ incorporated in azurin¹ enable the study of metal coordination geometries for both a mono- and a divalent state of the metal.

The overall structure of azurin consists of 8 β -strands forming a so-called β -barrel.² This is believed to make the protein highly rigid. The copper site is situated in a region formed by several β -strands and their connecting loops. Strong bonds are formed between the copper ion, the thiolate sulfur of Cys112, and the N δ -ring nitrogen in both His46 and His117 (see Figure 1). These three ligands form an irregular planar trigonal geometry. The sulfur of Met121 and the carbonyl oxygen in Gly45 approach the copper ion in axial positions to the trigonal plane (Figure 1 and Tables 1 and 2). Furthermore, the metal site coordination

geometry for azurin from *Alcaligenes denitrificans* was found by X-ray diffraction to be the same for Cu(I) and Cu(II)⁵ in contrast to EXAFS measurement on azurin from *Pseudomonas aeruginosa* where differences in the bond length for the two coordinating histidines were found.⁶ According to the concept of rack-induced bonding, the rigid protein structure forces the Cu(II) ion to adapt the special planar tricoordinated geometry characteristic of the type 1 copper.⁷ However, recent results indicate that, although the metal site is rigid, there is little difference in the energy between the coordination geometry for Cu(I) and Cu(II).⁸

In type 1 copper sites of most blue copper proteins, methionine is found at a distance from copper which is longer than normal binding distances. In azurin, the distance between the sulfur of Met121 and copper is 3.1 Å. Due to this unusual long distance it has been questioned whether it is a ligand or whether it has a structural role in the protein, and the function of Met121 has been intensively studied by site-directed mutagenesis.^{9,10}

Several spectroscopic techniques have been applied to azurin and mutants thereof in order to elucidate the interplay between the redox potential and the metal-coordination geometry for Cu(I) and Cu(II). Most prominent are EPR measurements and UV-vis absorption spectroscopy,^{11,12} but also EXAFS and resonance Raman spectroscopy have been applied.^{6,12} Spectroscopic techniques such as EPR, absorption spectroscopy, and

* Address correspondence to this author.

[†] Present address: Department of Chemistry, Royal Veterinary and Agricultural University, DK-1871 Frederiksberg C, Denmark.

[‡] Present address: Department of Biochemistry and Biophysics, Göteborg University, S-413 90 Göteborg, Sweden.

[§] Present address: Department of Physics, Guru Nanak Dev University, Amritsar, India.

[⊗] Abstract published in *Advance ACS Abstracts*, December 15, 1996.

(1) Danielsen, E.; Bauer, R.; Hemmingsen, L.; Andersen, M.-L.; Bjerrum, M. J.; Butz, T.; Troeger, W.; Canters, G. W.; Hoitink, G. W. G.; Karlsson, G.; Hansson, Ö.; Messerschmidt, A. *J. Biol. Chem.* **1995**, *270*, 573–580.

(2) Adman, E. T. In *Topics in molecular metalloproteins and structural biology*; Harrison, P. M., Ed.; Macmillan, New York, 1986; pp 1–42. Adman, E. T.; Jensen, L. H. *Isr. J. Chem.* **1981**, *21*, 8–12. Baker, E. N. *J. Mol. Biol.* **1988**, *203*, 1071–1095.

(3) Kraulis, P. J. *J. Appl. Crystallogr.* **1991**, *24*, 946–950.

(4) Nar, H.; Messerschmidt, A.; Huber, R.; van de Kamp, M.; Canters, G. W. *J. Mol. Biol.* **1991**, *221*, 765–772.

(5) Shepard, W. E. B.; Anderson, B. F.; Lewandowski, D. A.; Norris, G. E.; Baker, E. N. *J. Am. Chem. Soc.* **1990**, *112*, 7817–7819.

(6) Groeneveld, C. M.; Feiters, M. C.; Hasnain, S. S.; Rijn, J. van; Reedijk, J.; Canters, G. W. *Biochim. Biophys. Acta* **1986**, *873*, 214–227.

(7) Gray, H. B.; Malmström, B. G. *Comments Inorg. Chem.* **1983**, *2*, 203–209. Malmström, B. G. *Eur. J. Biochem.* **1994**, *223*, 711–718.

(8) Guckert, J. A.; Lowery, M. D.; Solomon, E. I. *J. Am. Chem. Soc.* **1995**, *117*, 2817–2844.

(9) Karlsson, B. G.; Aasa, R.; Malmström, B. G.; Lundberg, L. G. *FEBS Lett.* **1989**, *253*, 99–102.

(10) Karlsson, B. G.; Nordling, M.; Pascher, T.; Tsai, L.-C.; Sjölin, L.; Lundberg, L. G. *Protein Eng.* **1991**, *4*, 343–349.

(11) Pascher, T.; Karlsson, B. G.; Nordling, M.; Malmström, B. G.; Vänngård, T. *Eur. J. Biochem.* **1993**, *212*, 289–297.

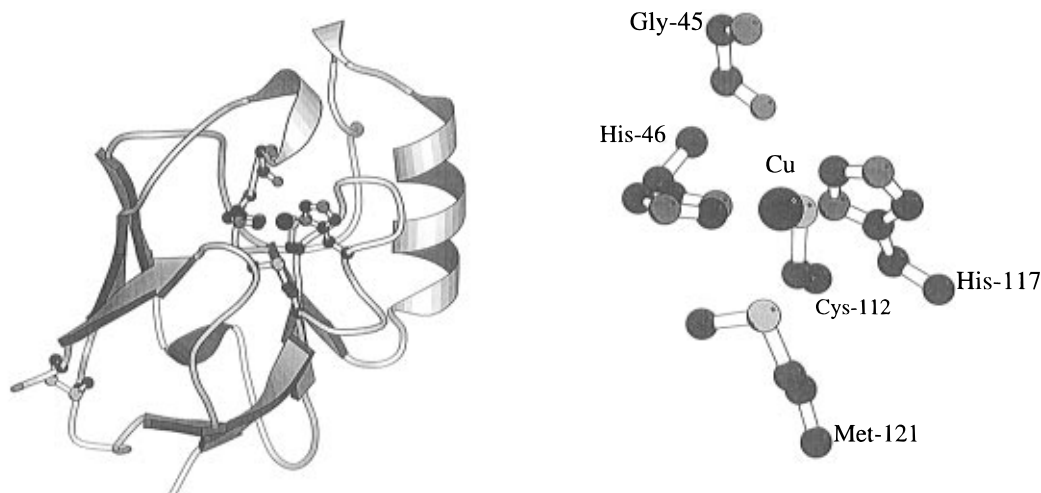


Figure 1. Schematic drawing of *Pseudomonas aeruginosa* azurin (left) and an enlarged view of the copper site (right). The view is from the solvent-exposed His-117 residue down through the β -barrel. A disulfide bridge is located at the lower left part of the molecule. The α -carbons and side chains of the amino acid residues in the copper site are shown except in the case of Gly-45 for which also the other backbone atoms are included. The residues have been labeled close to the α -carbons. The figure was drawn with MolScript³ using the structure of oxidized *Pseudomonas aeruginosa* azurin at pH 5.5.⁴

Table 1. Distances for the Coordination Sphere of Copper in Azurin *Pseudomonas aeruginosa* from X-ray Diffraction⁴

atoms involved	distance for Cu(II) ^a
Cu—O ₄₅	2.96
Cu—N ₁₁₇	2.04
Cu—N ₄₆	2.10
Cu—S ₁₁₂	2.26
Cu—S ₁₂₁	3.14

^a Taken as the average value from the structures for azurin from *Pseudomonas aeruginosa* determined from X-ray diffraction at pH 5.5 and 9.0.⁴

Table 2. Angles for the Coordination Sphere of Oxidized Copper in Azurin *Pseudomonas aeruginosa* from X-ray Diffraction⁴

atoms involved	angle ^a	atoms involved	angle ^a
O ₄₅ —Cu—N ₁₁₇	89	N ₁₁₇ —Cu—S ₁₁₂	123
O ₄₅ —Cu—N ₄₆	75	N ₁₁₇ —Cu—S ₁₂₁	88
O ₄₅ —Cu—S ₁₁₂	98	N ₄₆ —Cu—S ₁₁₂	134
O ₄₅ —Cu—S ₁₂₁	149	N ₄₆ —Cu—S ₁₂₁	76
N ₁₁₇ —Cu—N ₄₆	103	S ₁₁₂ —Cu—S ₁₂₁	110

^a Taken as the average value from the structures for azurin from *Pseudomonas aeruginosa* determined from X-ray diffraction at pH 5.5 and 9.0.⁴

resonance Raman spectroscopy monitor Cu(II). These spectroscopic techniques have been used to classify the state of the copper site as either type 1 or 2,² type 1 being represented by wild type (WT) azurin. Recently, experimental evidence showed that methionine was not in the electron transfer pathway.¹³ The Perturbed Angular Correlation of γ -rays (PAC) technique was recently introduced in the studies of small copper proteins such as azurin.^{1,14} In these applications cadmium has been used to substitute for copper in the protein. It was demonstrated that the coordination geometry of the cadmium ion in azurin is a tricoordinated planar geometry. It was further shown that Met121 mutants of azurin in several cases gave two coexisting metal-coordination geometries. In the case of Met121Ala and Met121Leu one of these was close to the WT

(12) Murphy, L. M.; Strange, R. W.; Karlsson, B. G.; Lundberg, L. G.; Pascher, T.; Reinhammar, B.; Hasnain, S. S. *Biochemistry* **1993**, *32*, 1965–1975.

(13) Langen, R.; Chang, I.-J.; Germanas, J. P.; Richards, J. H.; Winkler, J. R.; Gray, H. B. *Science* **1995**, *268*, 1733–1735.

(14) Danielsen, E.; Bauer, R.; Hemmingsen, L.; Bjerrum, M. J.; Butz, T.; Troeger, W.; Canters, G.; Den Blaauwen, T.; Van Pouderooyen, G. *Eur. J. Biochem.* **1995**, *233*, 554–560.

geometry. Despite the fact that ^{111m}Cd PAC studies showed that Cd(II), like Cu(II), has a tricoordinate geometry in wild type azurin, it is uncertain whether the range of different geometries existing for the cadmium-substituted Met121 mutants is relevant for Cu(I). For these reasons we have initiated studies on azurin and its mutant using ¹¹¹Ag(I) instead of ^{111m}Cd(II) as the PAC source. Thus a monovalent state with the same electronic configuration as Cu(I) is monitored in contrast to the divalent state of Cd(II). ¹¹¹Ag(I) has to our knowledge not before been used as a PAC probe in any published biological context but has previously been used to study metals and small inorganic complexes.¹⁵ It provides the possibility of monitoring the coordination geometry of a metal with the same electronic configuration and charge as Cu(I), a feature not easily accessible by most other spectroscopic techniques, because Cu(I) is in a closed shell electron configuration.

Materials and Methods

Preparation of Proteins. All chemicals were of analytical grade. Wild type and methionine mutants of azurin were isolated from *Escherichia coli* cells transformed with specific plasmids for the *Pseudomonas aeruginosa* azurin and its mutants.^{10,16} Apoproteins were prepared by dialysis for at least 12 h of approximately 1 mL of 0.5 mM copper protein in 0.1 M Tris pH 7.2 against 5 mL of the same buffer containing 0.1 M KCN. The KCN was removed by 3-fold dialysis against 100 mL of buffer, each dialysis lasting 24 h. All dialyses were done at 5 °C. To avoid problems with the formation of radiocolloidal particles between ¹¹¹Ag(I) and chloride ions both apo-WT-azurin and apo-met121leu-azurin were passed through a column containing Sephadex G25 equilibrated in 50 mM HEPES at pH 7.5. The apoproteins were frozen in liquid nitrogen and stored at –80 °C.

Production of ¹¹¹Ag(I) and Preparation of ¹¹¹Ag(I)-WT-Azurin and ¹¹¹Ag(I)-Met121Leu-Azurin. The PAC experiments performed in this study utilize ¹¹¹Ag with a half-life of 7.5 days. Twenty milligrams of 99.99% pure palladium foil (Aldrich) was irradiated by neutrons for 7 days at the 10 MW reactor at Research center Risø. The activity of ¹¹¹Ag 4 days after irradiation was about 400 MBq and a roughly equal activity of ¹⁰⁹Pd was observed. The palladium foil was dissolved in 1 mL of aqua regia (1/4 concentrated HNO₃ and 3/4 concentrated HCl) in a plastic tube. This solution was passed through a Dowex 1 strong anion exchange column, 0.9 cm ϕ and of 10 cm height equilibrated in 10 M HCl. The fractions containing ¹¹¹Ag(I)

(15) Haas, H.; Shirley, D. A. *J. Chem. Phys.* **1973**, *58*, 3339–3355.

(16) Karlsson, B. G.; Pascher, T.; Nordling, M.; Arvidsson, R. H. A.; Lundberg, L. G. *FEBS Lett.* **1989**, *246*, 211–217.

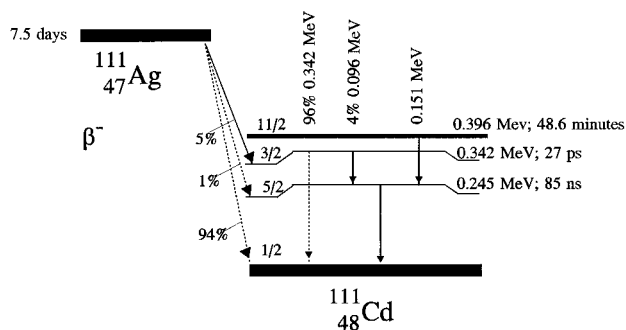


Figure 2. Schematic presentation of the decay of ^{111}Ag and $^{111\text{m}}\text{Cd}$. For each of the energy levels in ^{111}Cd the quantum number of the angular momentum (I), the energy, and the half-life are listed. Note that only 5% of the ^{111}Ag nuclei decay to the excited state in ^{111}Cd with angular momentum $3/2$, and of these only 4% decay through the double decay needed for PAC spectroscopy.

eluted in a peak of 5 mL showing no trace of palladium as monitored via the ^{109}Pd activity. Similarly all palladium was detected on the column when the flow was stopped shortly after all $^{111}\text{Ag}(\text{I})$ had passed. However, it could be seen by visual inspection that palladium slowly progresses through the column although much slower than ^{111}Ag . The 5 mL of 10 M HCl containing ^{111}Ag was evaporated to 50 μL in a glass tube. About 50% of the ^{111}Ag activity could be transferred to a test tube, the residual 50% being fixed in the glass beaker. To the transferred 50- μL solution was added 100 μL of 50 mM HEPES at pH 8.5 and the pH was adjusted to be between 6 and 7 with NaOH. Thirty microliters of this solution was added to 100 μL of 0.057 mM wild type apoazurin in 50 mM HEPES at pH 7.5 and 55 μL of this solution was added to 185 μL of 0.24 mM apoMet121Leu-azurin in 50 mM HEPES at pH 7.5. Both solutions were left at room temperature for 10 min for the metal to bind. Thereafter sucrose was added to a concentration of 55% in order to increase the viscosity. The final pH was 7.5 for the sample with WT-azurin and 7.4 for the sample with Met121Leu-azurin.

PAC Spectroscopy. The Perturbed Angular Correlations of γ -rays (PAC) technique is described in detail in the review by Frauenfelder and Steffen¹⁷ and with special emphasis on biological applications by Bauer.¹⁸

The decay schemes of the two isotopes ^{111}Ag and $^{111\text{m}}\text{Cd}$ are shown in Figure 2. By PAC the angular correlation of two γ -rays emitted in succession is measured as a function of the time between the two emissions. This angular correlation is affected by the hyperfine interaction of the nucleus in the intermediate state (here the 245-keV state in ^{111}Cd). In the case of no applied magnetic field the hyperfine interaction of the nucleus is due to the nuclear quadrupole interaction (NQI). It is through this interaction that the local surroundings of the nucleus are monitored.

In PAC the hyperfine interaction is monitored through its effect on the probability density, $W(\theta, t)$, of detecting the second γ -ray at an angle, θ , relative to the emission of the first γ -ray and at a time, t , after the first γ -ray

$$W(\theta, t) = \frac{e^{-t/\tau_N}}{4\pi\tau_N} (1 + A_2 G_2(t) P_2(\cos\theta)) \quad (1)$$

where τ_N is the lifetime of the intermediate level. Here the angular correlation has been separated into the angular dependence ($P_2(\cos\theta) = \frac{1}{2}(3\cos^2\theta - 1)$) and the time dependence (e^{-t/τ_N} and $G_2(t)$) (see below). The coefficient A_2 describes the anisotropy in the angular correlation between the two γ -rays. This anisotropy arises from the restriction in the direction of the angular momentum for the intermediate state due to the angular momentum carried away by the first γ -ray combined with the conservation of angular momentum. A_2 depends only on the nuclear decay and has the value 0.17 for ^{111}Cd and -0.18

(17) Frauenfelder, H.; Steffen, R. M. In *Alpha-, Beta- and Gamma-ray Spectroscopy*; Siegbahn, K., Ed.; North-Holland: Amsterdam, 1965; Vol. 2, pp 97–1198.

(18) Bauer, R. Q. *Rev. Biophys.* **1985**, *18*, 1–64.

for ^{111}Ag .¹⁵ In an actual experiment the solid angles of the detectors and the size of the sample decrease these values numerically. The perturbation function $G_2(t)$ describes the time evolution of the probability of detecting the second γ -ray at time t . If no interaction with the surroundings is present, which would be the case if the nucleus is surrounded by an isotropic charge distribution, then $G_2(t)$ is independent of time and equal to 1, i.e. full anisotropy is conserved in time. For a NQI constant in time the perturbation function $G_2(t)$ will oscillate in time. A time-dependent NQI will typically arise because of thermal interaction with the surroundings and lead to the loss of anisotropy making $G_2(t)$ approach 0, while reaching thermal equilibrium.

The PAC spectrometer consists of 6 BaF_2 -scintillator detectors with conical fronts arranged such that each detector is situated at the face center of an imaginary cube. The sample is positioned at the center of this cube. Thus pairs of detectors form either 180° or 90° detector-sample-detector angles. The spectrometer is a built-out version of the "PAC-camera" described previously.¹⁹ The temperature of the sample was controlled within 2°C by a Peltier element.

With this spectrometer $W(\theta, t)$ can be measured through the time-resolved coincidence spectra between pairs of detectors. In total 6 combinations with $\theta = 180^\circ$ and 24 combinations with $\theta = 90^\circ$ are collected simultaneously. Before $G_2(t)$ can be derived from $W(\theta, t)$ the spectra must be corrected for a background due to accidental coincidences, and time equal zero must be found for all 30 spectra. Time resolution and zero-point adjustment were determined using the large prompt in the spectra due to the intense 342-keV γ -ray detected in two counters simultaneously by Compton scattering. The time resolution was about 1 ns (full width at half maximum) at the energies of ^{111}Ag . The perturbation function is then formed by:

$$A_2 G_2(t) = 2 \frac{W(180^\circ, t) - W(90^\circ, t)}{W(180^\circ, t) + 2W(90^\circ, t)} \quad (2)$$

where $W(180^\circ, t)$ denotes the geometric average of the 180° spectra, and $W(90^\circ, t)$ denotes the geometric average of the 90° spectra. This procedure minimizes the effect of different efficiency for the 6 detectors.

From Figure 2 it can be seen that only 0.2% of the radioactive ^{111}Ag decays through the emission of two successive γ -rays. It is this minor fraction of the activity that can be used for PAC. This could be the reason why the isotope has not so far been used in biochemical studies. However, the improvement in the signal to noise by selecting only coincidence counts together with the long half-life of ^{111}Ag (7.5 days) makes it possible, as in the present work, to obtain high-quality spectra. The acquisition time for the ^{111}Ag PAC spectra presented here was typically 24 h.

Nuclear Quadrupole Interaction. Static Case. The NQI is the interaction of the electric quadrupole moment of the nucleus (in the intermediate state) and the electric field gradient, V_{ij} where i, j refer to Cartesian coordinate axis x, y , or z . It is important to note here that the intermediate state is the same in the two different decays of ^{111}Ag and ^{111}Cd . Therefore differences in the nuclear quadrupole interactions between the two must reflect differences in the electric field gradient. For a known charge density the electric field gradient tensor is found as:

$$V_{ij} = \int \frac{\rho(\vec{r})k}{r^3} (3\alpha_i\alpha_j - \delta_{ij}) dV \quad (3)$$

where i and j refer to any of the axes x, y , and z , and $\rho(\vec{r})$ is the surrounding charge density at the point $\vec{r} = (r_x, r_y, r_z)$. α_i is the direction cosine r_i/r ($\alpha_x = \cos\phi \sin\theta$, $\alpha_y = \sin\phi \sin\theta$, and $\alpha_z = \cos\theta$, where θ and ϕ are the polar and azimuthal angles at the position (r_x, r_y, r_z)), k is Coulombs constant, and $dV = dr_x dr_y dr_z$. Equation 3 illustrates that the NQI is sensitive to both the angular (through θ and ϕ) as well as the radial (through r^{-3}) distribution of charges.

For randomly oriented molecules the orientation of the electric field gradient with respect to the protein cannot be determined. Thereby it is only possible to determine the diagonal elements of the tensor after diagonalization. Note that the sum $V_{xx} + V_{yy} + V_{zz}$ is equal to 0. The electric field gradient is therefore parametrized by the largest

(19) Butz, T.; Saibene, S.; Fraenzke, T.; Weber, M. *Nucl. Instrum. Methods Phys. Res.* **1989**, *A284*, 417–421.

Table 3. NQI for WT Azurin and Met121Leu Mutant of Azurin at 1 °C

protein	η	$ \omega_0 $ (Mrad/s)	ω_{yy} (Mrad/s)	$\Delta\omega_0/\omega_0$	τ_c (ns)	% ^d
WT(silver) ^a	0.507 ± 0.004	343.3 ± 0.7	258.7	0.014 ± 0.004	139 ± 30	100
WT(cadmium) ^b	0.522 ± 0.001	337.7 ± 0.2	257.0	0.010 ± 0.001	200 ± 20	100
Met121Leu(silver) ^a	0.476 ± 0.003	336.2 ± 0.4	248.1	0.006 ± 0.003	118 ± 12	100
Met121Leu(cadmium) ^b	0.485 ± 0.004	332.3 ± 0.6	246.7	0.014 ± 0.002	200 ^c	48
Met121Leu(cadmium) ^b	0.730 ± 0.010	264.0 ± 2.0	228.4	0.071 ± 0.001	200 ^c	52

^a This work. ^b Danielsen et al.¹ ^c f means the parameter is fixed. ^d Population of the site in percentage.

diagonal element, $|V_{zz}|$, after diagonalization, and the asymmetry parameter,

$$\eta = \frac{|V_{xx} - V_{yy}|}{|V_{zz}|} \quad (4)$$

where V_{xx} and V_{yy} refer to the other two diagonal elements of the diagonalized electric field gradient tensor.

A non-vanishing electric field gradient will split the intermediate state with angular momentum $5/2$ into only 3 and not 6 sublevels because of the inversion symmetry of the NQI. From this hyperfine splitting the two parameters $|V_{zz}|$ and η can be determined.¹⁸ In the case of identical, static, and randomly oriented molecules, the perturbation function $G_2(t)$ (see eq 1) is¹⁸

$$G_2(t) = a_0 + a_1 \cos(\omega_1 t) + a_2 \cos(\omega_2 t) + a_3 \cos(\omega_3 t) \quad (5)$$

The frequencies are seen directly in the Fourier transformed PAC spectra and each of them correspond to an energy difference, ΔE_i , in the hyperfine splitting of the intermediate state by the relation $\omega_i = 2\pi\Delta E_i/h$, where h is Planck's constant. Each frequency is proportional to $|V_{zz}|$ with a proportionality constant depending on η . The four amplitudes, a_0, \dots, a_3 , also depend on η and sum to 1 in order to make $G_2(t) = 1$ for $t = 0$ to ensure full anisotropy. Thus from the time dependency of $G_2(t)$, $|V_{zz}|$ and η can be determined through least-squares fitting.¹⁸ Since the energy differences do not only depend on the electric field gradient but also on the angular momentum and quadrupole moment (Q) of the intermediate state of the nucleus, it is advantageous to relate the experimental results to the nuclear quadrupole interaction tensor:

$$\omega_{ij} = \frac{12\pi|eQ|}{40h} |V_{ij}| \quad (6)$$

where h is Planck's constant. The numerical value of the largest diagonal element after diagonalization is then denoted ω_0 , and η is unchanged.

Effects of a Dynamic Electric Field Gradient. In the present case the nuclear quadrupole interaction can be time dependent in at least two ways. First there is the reorientation of the protein, and thereby of the electric field gradient, caused by the rotational diffusion. This has the consequence that $G_2(t)$ will converge to 0 as a function of time representing thermal equilibrium and isotropy in the angular correlation between the two γ -rays. The effect of rotational diffusion is described in Danielsen and Bauer.²⁰ As the correlation time, τ_c , is much longer than $(\omega_0)^{-1}$ (see Table 3), the dynamic perturbation function $G_2(t, \tau_c)$ can be expressed in terms of the static perturbation function $G_2(t)$ as $G_2(t, \tau_c) = \exp(-t/\tau_c) G_2(t)$.²⁰

A second way that the nuclear quadrupole interaction can be time dependent is related to the decay of ^{111}Ag to ^{111}Cd . The β -decay leads to a decay from a Ag(I) ion to a Cd(II) ion. Eventually, the coordination geometry for Ag(I) achieved before the β -decay must change to the coordination geometry for Cd(II) (if different from Ag(I)) after the β -decay. If the time constant for this transformation is much larger than the 200 ns observed in the PAC spectrum, the PAC spectrum will be characterized by the NQI for the coordination geometry for Ag(I). Similarly, if the time constant for the transformation is much shorter than a few nanoseconds, the PAC spectrum will be characterized by the NQI for the coordination geometry for Cd(II). Finally, for time constants in the range of 10 to 100 ns, a dynamic PAC spectrum will appear representing the change between the two coordination geom-

etries. The recoil of the cadmium nucleus from the emission of the β -particle could also produce dynamic effects in the PAC spectrum.

Angular Overlap Model Calculations of NQI. In the interpretation of the measured NQI's we have used the Angular Overlap Model (AOM)²¹ in which the contribution to the electric field gradient from a specific ligand is assumed to be axially symmetric with respect to the ligand-metal bond direction, independent of the other ligands and (within normal bonding distances) also independent of the bonding length. Under these assumptions the independent contributions from different ligands, denoted partial NQI parameters, have been determined from model complexes.²¹ Thus, for example a coordinating nitrogen in a histidine residue is assigned a unique partial NQI parameter. The NQI tensor can then be calculated as a sum over contributions from the different ligands:

$$\omega_{ij} = \frac{1}{2} \sum_l \omega_l (3\alpha_{il}\alpha_{jl} - \delta_{ij}) \quad (7)$$

where i, j again is any of the three axes x, y , and z , α_{il} is the direction cosine i in the direction from the center of the metal ion to the l 'th ligand, and ω_l is the l 'th ligands partial NQI parameter. As described above in relation to eq 3, ω_0 and η are obtained by diagonalization of the tensor in eq 7.

The model calculations are treated in detail in Danielsen et al.¹⁴ with special emphasis on a three-coordinated structure of two histidines and one cysteine. With typical experimental uncertainties the technique is sensitive to changes in ligand-metal-ligand angles of only a few degrees. It is important to note that for a specific ligand, differences in ligand-metal distance are ignored. The reason for this is twofold, first it was demonstrated in Bauer et al.²¹ that different ligands could be assigned the same partial NQI independent of the bonding distance within 0.2 Å. Second, assuming independency of partial NQI's parameters for the same ligand from one complex to another is necessary, since a given coordination geometry only results in two experimentally determined parameters, ω_0 and η . Thus differences are interpreted in terms of geometry and types of ligands.

NQI Determination from $^{111}\text{Ag(I)}$ -WT-Azurin PAC Spectra. The function $A_2 G_2(t)$ was analyzed by conventional least- χ^2 fitting routines. Each NQI is described by the following parameters: ω_0 , η , $\Delta\omega_0/\omega_0$, τ_c , and A_2 . $\Delta\omega_0/\omega_0$ is used for describing small inhomogeneities in ω_0 due to variations from one molecule to another with respect to conformations of the probe sites. It is assumed that the variations can be described by identical asymmetry parameters, η , and a Gaussian distribution of ω_0 with the width $\Delta\omega_0$. Thus, deviations from zero indicate that the ^{111}Ag or ^{111m}Cd nuclei are subjected to a distribution of surroundings. In general, shifts in angular position of a ligand by only a few degrees will be quite enough to show up as a frequency distribution of a few percent. τ_c is the correlation time of the rotational diffusion induced by the Brownian motion. For a rigid spherical molecule with volume V , embedded in a solution with viscosity ξ , the correlation time is $\tau_c = \xi V/(kT)$, where k is Boltzmann's constant and T is the absolute temperature.

The AOM²¹ was used to estimate the changes between the different geometries around the metal ion. The input parameters to the AOM were the partial nuclear quadrupole interactions of the different ligands and the angular positions of the ligands. A calculation was carried out in which all of the experimental NQIs were assumed to be due to three-coordination by one cysteine and two histidines, with the exception

(21) Bauer, R.; Jensen, S. J.; Schmidt-Nielsen, B. *Hyperfine Interact.* **1988**, *39*, 203–234. Bauer, R.; Christensen, C.; Larsen, E. *J. Chem. Phys.* **1979**, *70*, 4117–4122.

(20) Danielsen, E.; Bauer, R. *Hyperfine Interact.* **1992**, *62*, 311–324.

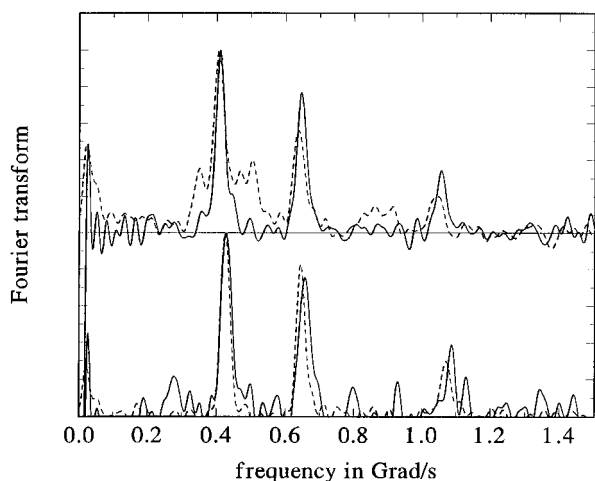


Figure 3. Fourier transformation of PAC spectra: dotted line ^{111}mCd (from Danielsen et al.)¹ and solid line ^{111}Ag ; lower panel WT and upper panel Met121Leu mutant. Although the PAC spectra from ^{111}Ag have negative amplitudes in the Fourier transform we have multiplied the Fourier transforms for ^{111}Ag by -1 in order to make a comparison with the Fourier transforms for ^{111}mCd easier.

of the NQI of cadmium-substituted Met121Leu azurin which is very broad, and which has previously been suggested to be due to an additional coordinating water.¹ In order to isolate the effects of geometrical changes, it was further assumed that the changes in the observed ω_0 and η were due to changes in ligand positions only. It was required that the calculated ω_0 should not differ from the experimental ω_0 by more than 1 Mrad/s and the difference for η should not be more than 0.005. The partial NQIs of histidine were fixed at 100 Mrad/s and of cysteine at 317 Mrad/s. This is approximately 5% more than the partial NQIs determined from 5- and 6-coordinated model complexes but within the uncertainty²¹ and makes it possible to get within the range of the experimental values for all four complexes.

Results

PAC spectra have been obtained from $^{111}\text{Ag(I)}$ -WT-azurin and from $^{111}\text{Ag(I)}$ -Met121Leu-azurin at pH 7.5 at 1 and 25 °C. Fourier transformations of PAC spectra from $^{111}\text{Ag(I)}$ -WT-azurin and from $^{111}\text{Ag(I)}$ -Met121Leu-azurin at pH 7.5 at 1 °C are shown in Figure 3 together with the corresponding $^{111}\text{mCd(II)}$ derivatives. The derived NQI's from least-squares fitting to the PAC spectrum $A_2 G_2(t)$ at 1 °C are given in Table 3 where NQI's for corresponding $^{111}\text{mCd(II)}$ derivatives are also given for comparison. From Table 3 it can be seen that ω_0 and η from $^{111}\text{Ag(I)}$ -WT-azurin and $^{111}\text{mCd(II)}$ -WT-azurin are different, but the differences in ω_0 and η are so small that it is likely that the two geometries differ by no more than a degree in each ligand–metal–ligand angle. For the Met121Leu mutant the Fourier transform of the PAC spectrum from the $^{111}\text{Ag(I)}$ derivative shows only one NQI in contrast to the $^{111}\text{mCd(II)}$ derivative where the spectrum is composed of two NQI's (Figure 3).

In order to see whether there was any effect in time of decay from $^{111}\text{Ag(I)}$ to $^{111}\text{mCd(II)}$, the spectra at 1 °C together with the spectra at 25 °C were divided into two time windows. These were analyzed by fixing all parameters other than ω_0 and η at the value determined from the time range covered by both windows. The results are shown in Table 4. ω_0 determined from $^{111}\text{Ag(I)}$ -WT-azurin is significantly different in the first 55–65 ns as compared to the next 45–55 ns and the tendency at both temperatures is a relaxation toward ω_0 for $^{111}\text{mCd(II)}$ -WT-azurin. At 25 °C this relaxation toward the Cd(II) geometry is completed with a half-life on the order of 50 ns. No significant change with either temperature or time occurs for the mutant (Table 4).

Table 4. Temperature and Time Dependency of NQI for WT Azurin and Met121Leu Mutant of Azurin

	η	ω_0 (Mrad/s)	time interval (ns)	temp (°C)
WT(silver)	0.504 ± 0.007	345.0 ± 1.0	9–65	1
WT(silver)	0.513 ± 0.004	340.8 ± 0.7	65–121	1
WT(silver)	0.529 ± 0.008	344.0 ± 1.2	9–54	25
WT(silver)	0.537 ± 0.007	338.4 ± 0.9	54–99	25
Met121Leu(silver)	0.474 ± 0.004	336.8 ± 0.5	9–65	1
Met121Leu(silver)	0.479 ± 0.002	335.8 ± 0.3	65–121	1
Met121Leu(silver)	0.481 ± 0.005	337.2 ± 0.7	9–54	25
Met121Leu(silver)	0.474 ± 0.002	336.7 ± 0.4	54–99	25

Table 5. Fit to the Time Dependency of the NQI Detected in the PAC Spectra for $^{111}\text{Ag(I)}$ -WT-Azurin at 1 and 25 °C^a

temp (°C)	$\Delta\omega$ (Mrad/s)	k ($\text{s}^{-1} \times 10^{-6}$)
1	8.8 ± 2.5	10.9 ± 5.2
25	10.5 ± 3.7	18.2 ± 8.1

^a The values of ω_0 and ω_{yy} were fixed to those for $^{111}\text{mCd(II)}$ -WT-azurin.

After establishing a time dependency of the NQI parameters for the wild type, the spectra from $^{111}\text{Ag(I)}$ -WT-azurin at 1 and 25 °C were analyzed with the following model for ω_0 , keeping ω_{yy} constant, in $A_2 G_2(t)$:

$$\omega_0(t) = \Delta\omega e^{-kt} + 337.7 \quad (8)$$

where 337.7 is the value for ω_0 for $^{111}\text{mCd(II)}$ -WT-azurin. This assumes that the process is of first order in time. The results shown in Table 5 give a ratio of 1.7 ± 1.0 between the rate constants obtained at the two temperatures. This corresponds to an activation barrier of less than 30 kJ/mol. The derived parameter¹⁴ $|\omega_{yy}| = (\eta + 1)/2 \omega_0$ is also listed in Table 3. This parameter is subject to much smaller relative changes than ω_0 , indicating that the change in geometry is mostly in-plane.¹⁴

The AOM calculations show that the NQI is most sensitive to the angle between the two histidines and the sum of the three ligand–metal–ligand angles, which is an indicator of how planar the structure is. The result of the calculation is that the difference between Ag-wt-azurin and Cd-wt-azurin can be ascribed to as little as an increase in the His–metal–His angle by 1.6° and a decrease in the angle sum by only 0.5° in going from Ag to Cd. The change from Ag-wt-azurin to Ag-met121leu-azurin can be accounted for by decreasing all of the ligand–metal–ligand angles by 1–2° with a total decrease of the sum by 4.5°, so that the structure in this case is less planar. A similar tendency is seen for the change from Cd-wt-azurin to Cd-Met121Leu-azurin, with the exception that for cadmium there is also the occurrence of a very different NQI, suggested to be due to the binding of a water ligand.¹

Discussion

Cu(I) and Ag(I) are both monovalent, and have a d^{10} electron configuration. Consequently, these two ions behave very similarly, apart from the larger ionic radius of Ag(I) (1.26 Å as compared to 0.96 Å for Cu(I)). Cd(II) is divalent as is Cu(II), but has also a d^{10} electron configuration, in contrast to Cu(II). In wild type azurin the copper site is, according to the theory of rack-induced bonding, assumed to have a rigid coordination geometry defined by the protein and the metal site ligands.⁷ The PAC experiments on $^{111}\text{Ag(I)}$ -substituted, as well as $^{111}\text{mCd(II)}$ -substituted,¹ azurins show that the metal site coordination geometry is very rigid and similar to WT azurin containing copper. As the NQI's for WT azurin with both $^{111}\text{Ag(I)}$ and $^{111}\text{mCd(II)}$ are very similar and can be calculated

from the geometry from X-ray diffraction studies and as the geometries for Cu(I) and Cu(II) are also very similar⁵ then Cu(I), Cu(II), Ag(I), and Cd(II) occupy almost the same coordination geometry in wild type azurin.

The β -emission of ^{111}Ag results in a recoil energy for the ^{111}Cd nuclei of less than 330 kJ/mol. This translative movement of the cadmium nucleus is expected to be dissipated within a nanosecond after β -emission whereby no effect of the recoil should be observable in the PAC spectrum. This is supported by the sharp peaks observed in the Fourier transformation of the PAC spectra for ^{111}Ag -azurin. That a change from a Cu(I) to a Cu(II) environment in azurin can be fast is further demonstrated in Wiesenfeld et al.²² where reappearance of the charge transfer band after ultrafast reduction of Cu(II) occurs within 2 ps.

The fact that $^{111}\text{Ag(I)}$, before the β particle is emitted, is a Ag(I) ion, whereas after the β emission it is a Cd(II) ion, can be used to investigate the dynamic of this transformation. If the coordination geometry of Ag(I) relaxes to the coordination geometry of Cd(II) with a time constant which is much longer than 100 ns, the time span of ^{111m}Cd and ^{111}Ag PAC spectra, then the spectrum will be characteristic of Ag(I). If, however, the time constant is much shorter than 100 ns only the coordination geometry of Cd(II) will be observed.

From Table 4 it is seen that the NQI for $^{111}\text{Ag(I)}$ -WT-azurin changes as a function of both time and temperature such that the NQI of $^{111m}\text{Cd(II)}$ -WT-azurin (Table 3) is reached after about 100 ns at 25 °C. For the $^{111}\text{Ag(I)}$ -Met121Leu mutant the NQI is different from that which is closest to the wild type of the cadmium-substituted Met121Leu mutant at both 1 and 25 °C throughout the time range analyzed (Table 4). This shows that for the $^{111}\text{Ag(I)}$ -Met121Leu mutant at both 1 and 25 °C we are monitoring a Ag(I) geometry and that for $^{111}\text{Ag(I)}$ -WT-azurin at 1 °C we are also monitoring a Ag(I) geometry. The time-dependent model for the NQI (results in Table 5) shows that the activation energy for the transition between the Ag(I) geometry and the Cd(II) geometry is small. Furthermore, the AOM calculations show that for the wild type there is only a need for a geometrical adjustment of a few degrees when changing from Ag(I) to Cd(II). This is in agreement with the calculation presented in Guckert et al.⁸ showing that there is no need for a structural rearrangement required for the transition between Cu(I) and Cu(II) when Cu(I) adopts the geometry found in plastocyanin and azurin.

In most blue copper proteins a methionine is found in an axial position to the two histidines and cysteine ligands relatively close to the metal, and, therefore, the possible function of this conserved amino acid has attracted some attention.^{9,12,13} In $^{111}\text{Ag(I)}$ -substituted Met121Leu azurin the metal site coordination geometry is found to be similar to that of WT azurin. That is, even with the copper exchanged by the monovalent silver and with the methionine exchanged with leucine, the protein is capable of maintaining the same, well-defined metal site

structure. In contrast to ^{111}Ag , $^{111m}\text{Cd(II)}$ -substituted Met121Leu azurin showed two coexisting molecular species, one with a coordination geometry similar to WT azurin and one, very flexible, distinctly different from WT azurin. Thus, when copper is exchanged with cadmium, which is divalent, there is a significant fraction of the protein molecules which are no longer capable of keeping the WT coordination geometry. The alternative metal geometry is suggested to be due to an increase in the coordination number by the addition of a water ligand.¹ In the Met121Leu mutant there are differences in the metal coordination geometry, depending on the oxidation state of the metal: The coordination geometry for the metal ion in the monovalent state is very similar to that of WT azurin whereas the coordination geometry for the metal ion in the divalent state changes to a new more flexible metal site for about 50% of the protein molecules.¹

EPR and redox potential measurements have been performed on the WT azurin and on the Met121Leu mutant.^{11,12} The redox potential as well as the hyperfine splitting parameter *A* from EPR experiments change upon mutation, whereas only insignificant changes occur in the EPR *g* parameters. The latter implies that the coordination geometry on Cu(II) does not change very much for the mutant relative to WT, whereas the changes in *A* support some structural changes. The changes in redox potential may be caused by changes in the coordination geometry of both Cu(I) and Cu(II). Based on the PAC results we suggest that the coordination geometry of Cu(I) does not change significantly upon mutation of Met121 to Leucine, but that the coordination geometry of Cu(II) for a fraction of the protein molecules becomes very flexible and changes coordination geometry. The function of methionine 121 could thus be to keep the rigid well-defined coordination geometry for both Cu(I) and Cu(II) in particular by excluding water from binding to Cu(II).

The present work demonstrates for the first time that it is possible via PAC spectroscopy to study selectively the monovalent and divalent state for a metal ion in a metal binding protein. It also shows that important biological information can be obtained using the much more accessible PAC isotope ^{111}Ag , with a half-life of 7.5 days relative to the 49-min half-life of ^{111m}Cd . Furthermore, dynamic processes resulting from the change from Ag(I) to Cd(II) (because of the nuclear decay) occurring on a nanosecond time scale may be monitored. Potentially, PAC spectroscopy may be applied to study whether the interaction of blue copper proteins with their physiological partners in solution depends on the oxidation state of the metal ion.

Acknowledgment. The present work has been supported by the Danish Natural Research Council via the Center for Bioinorganic Chemistry. The authors are indebted to Professor Tilman Butz for much helpful advice concerning ^{111}Ag PAC spectroscopy, to Marianne Lund Jensen for excellent help with sample preparations, and to Dr. Göran Karlsson for providing us with wild type azurin and the Met121Leu mutant.

(22) Wiesenfeld, J. M.; Ippen, E. P.; Corin, A.; Bersohn, R. *J. Am. Chem. Soc.* **1980**, *102*, 7256–7258.